

Interpretation of x-ray magnetic circular dichroism and x-ray absorption near-edge structure in Ni

A. I. Nesvizhskii,¹ A. L. Ankudinov,¹ J. J. Rehr,¹ and K. Baberschke^{1,2*}

¹*Department of Physics, University of Washington, Seattle, Washington 98195*

²*SSRL, SLAC, Stanford University, Stanford, California 94309*

(Received 12 September 2000)

An interpretation of the spectral features in the Ni L_3 x-ray absorption near-edge structure and x-ray magnetic circular dichroism signals is presented, based on both one-electron multiple-scattering and atomic-multiplet calculations. Neither of these approaches is fully satisfactory. Although most of the observed features are reproduced by one-electron calculations, the pronounced peak about 3 eV above the edge is not. Conversely, the peak at 6 eV and the smooth plateau just beyond are not reproduced by the multiplet calculations. The lack of the 3-eV feature is attributed to the neglect of many-body effects in the interaction between core hole and final-state d^n configuration. The observed negative plateau between L_3 and L_2 edges is attributed to transitions to spin-polarized continuum ϵd states, and the 6-eV peak, to multiple scattering paths of intermediate range and disappears for Ni clusters smaller than 13 atoms. The necessity of both one-electron and atomic-multiplet calculations to explain all features in the data demonstrates the need for a combined approach.

I. INTRODUCTION

X-ray magnetic circular dichroism (XMCD) and x-ray absorption near-edge structure (XANES) are powerful, element-specific tools for obtaining information about magnetic systems. Various XANES and XMCD sum rules have often been used to investigate spin and orbital moments in $3d$ transition metals.¹ In this paper, we use theoretical calculations to interpret the various spectral features in XANES and XMCD at the Ni $L_{2,3}$ edges. Ni is a particularly instructive case for comparing theory and experiment among $3d$ elements, because the L_2 and L_3 edges are well separated by about 17.5 eV, the maximum separation possible for ferromagnetic $3d$ metals. This separation permits a detailed investigation of the region between the edges, where several interesting features are observed.

XANES and XMCD of Ni $L_{2,3}$ edges have been studied previously both for bulk Ni (Refs. 2–4) and for films.^{5–9} For example, these spectra have been used to investigate changes in electronic structure as a function of film thickness in Ni/Cu,⁵ Ni/Fe,⁶ Ni/Co/Cu,⁷ and Ni/Pt (Ref. 8) films. Similarly, modification of the electronic structure by stepwise oxidation has been investigated.⁹ Several interesting features are observed in the XMCD signal, including an extended negative plateau between the L_2 and L_3 edges, and notable satellite structures at 3 and 6 eV above the L_3 edge. However, an unambiguous interpretation of these features has been lacking. For example, it is not clear whether the shape and area of the L_3 white line in x-ray absorption spectra (XAS) is determined only by one-electron processes or whether multiplet transitions and other many-particle excitations^{10–12} also contribute to the overall intensity. To answer these questions it is important to understand the absorption cross section in detail and to evaluate separately the contributions from single- and many-particle excitations.

Several different approaches are currently used to calculate XAS, each of which stresses different aspects of the electronic structure. In the present paper we use both

atomic-multiplet^{13,14} (AM) and real space multiple scattering (RSMS) calculations.^{15–17} AM calculations generally reproduce experimental results close to the $L_{2,3}$ edges of transition metals.¹⁴ However, the AM theory quickly becomes less reliable several eV away from the edges. For example, attempts to interpret the 6-eV satellite in terms of multiplet effects^{7,13,14} were inconclusive. Within the AM approach, the treatment of the atomic environment is greatly simplified, and usually reduced to one or more crystal-field parameters determined by fitting to experiment. In addition, this approach contains only localized atomic orbitals and, therefore, fails to reproduce the XANES above about 6 eV of the edge, where the contribution from transitions to delocalized (i.e., continuum) d states is dominant. On the other hand, the *ab initio* RSMS approach treats the atomic environment in terms of multiple scattering without adjustable parameters, and generally gives good agreement with experiment for $3d$ transition metals, except very close to the edge. As discussed previously,^{10,17,18} the 6-eV satellite in XANES is reproduced by one-electron calculations. In particular, this peak has been attributed to a critical point in the band structure, and is therefore associated with multiple scattering. In this paper, we reanalyze all spectral features observed in high-resolution experimental data using both AM and RSMS (Ref. 16) calculations, and thereby derive an interpretation that encompasses both single-electron theory and many-body multiplet effects.

II. THEORY

The x-ray absorption coefficient can formally be obtained from Fermi's golden rule:

$$\mu_j^\epsilon(E) \sim \left\langle \left| I \left| \sum_{i,F} \vec{\alpha}_i \cdot \vec{\epsilon} e^{i\vec{k} \cdot \vec{r}} \right| F \right|^2 \right\rangle \delta(E - E_F + E_I), \quad (1)$$

where $|I\rangle$ and $|F\rangle$ are many-body N particle wave functions for the initial (I) and final (F) states of the system. For an

atomic system one can calculate approximate many-body states, e.g., as linear combinations of Slater determinants. For high-energy continuum states, the atomic calculations are well represented with a separable approximation: i.e., the final N particle wave function $|F\rangle = |f\rangle|F'_{N-1}\rangle$ is a product of a single-electron photoelectron wave function $|f\rangle$ and an $N-1$ particle wave function $|F'\rangle$, where the prime denotes quantities in the presence of a core hole. This approximation works well far above threshold, but ignores the effect of neighboring atoms and many-body effects. However, these problems can be corrected for by including various multiplet states and by introducing crystal fields to simulate the effect of the environment. In this paper we use the AM code of de Groot¹⁴ to treat such effects.

On the other hand, multiatom, one-electron theories (e.g., band structure or RSMS) account well for the effect of the environment on the final-state wave function $|f\rangle$ without any parameters, but usually neglect multiplet splitting effects. In this paper we use the real space Green's-function code¹⁶ FEFF8. In the RSGF method the x-ray absorption coefficient μ_j^ϵ for a given edge j and polarization ϵ can be obtained from the spin-dependent, one-electron density matrix $\hat{\rho}(x, x', E) = \text{Im} G(x', x, E)$,

$$\mu_j^\epsilon(E) \sim \langle j | \hat{\epsilon}^* \cdot \vec{r}' \hat{\rho}(x, x', E) \hat{\epsilon} \cdot \vec{r} | j \rangle \theta(E - E_F), \quad (2)$$

where $|j\rangle$ is the core state, E_F is the Fermi energy, $\hat{\epsilon}$ is the x-ray polarization vector, and $x = (\vec{r}, s)$ denotes space and spin variables. In this approach the full Green's function $G(x', x, E)$ naturally separates into central atom and multiple-scattering terms, and is calculated including spin and spin-orbit interactions using an interpolative approach.¹⁹

The *ab initio* self-consistent FEFF8 code has a number of advantages. It naturally includes final-state broadening due to core hole lifetime and photoelectron self-energy shifts. In addition, the code permits quantitative calculations of XAS up to very high energies (of order 1000 eV above threshold), while traditional band-structure codes usually are limited to 20–30 eV above the edge. Its disadvantages are that the code is based on an effective one-electron calculation with muffin-tin potentials and all many-body effects lumped into an approximate self-energy. The calculations here are carried out for initial (ground) state potentials, rather than with a core hole. For 3d transition metals and systems with more than half-filled d bands, such initial-state calculations usually give better agreement with experiment than calculations done with final-state potentials (fully screened core hole)²⁰ and represent important exceptions to the ‘‘final-state rule,’’ i.e., the prescription that one-electron calculations of XAS should be carried out in the presence of a core hole. Such exceptions are not unexpected for systems with a nearly completely filled band.²²

III. RESULTS AND DISCUSSION

Figure 1 shows the Ni $L_{2,3}$ XANES obtained from experiment and from both AM and RSMS theory. Although the overall shape is reasonable agreement, the amplitude discrepancies are due mostly to the approximate treatment of Debye-Waller factors in the calculations. These AM results are based on a single d^8 configuration and only take into

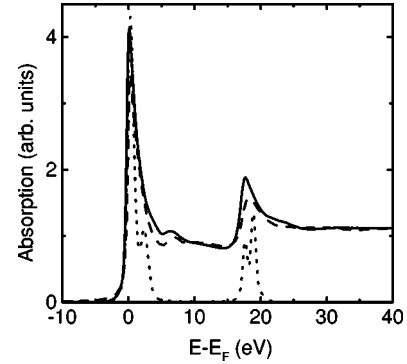


FIG. 1. $L_{2,3}$ edge XANES, as calculated by RSMS (dashes) and AM theory (dots) and from experiment (solid).

account contributions from localized atomic states. The 3-eV satellite is clearly seen in the AM calculations, and corresponds to the asymmetric shape (or shoulder) on the white line of the of experimental XAS.

The XMCD signal calculated by FEFF8 for a cluster of 50 atoms and measured in experiment are shown in Fig. 2. A bigger cluster does not produce any significant changes, but for a 13-atom cluster (dotted curve in inset) with only a single coordination shell, the 6-eV feature is missing. Ni L -shell XANES and XMCD in films has been studied in various works.^{5,7} The overall agreement between experiment and theory for XMCD is good, except that again (Fig. 2) the RSGF calculations miss the 3-eV peak. From Fig. 1 it is clear that such a peak can arise from AM splitting of the main peak. Hence this appears to be a many-body feature that one cannot expect to obtain from broadened one-electron calculations. The intensity of the main peak or white line dominates the sum rules for orbital and spin moments, and hence the integrated intensity of the white line in XMCD is roughly proportional to the spin moment.

In some works, both the 3-eV and 6-eV satellites have been assigned to multiplets.⁷ In this interpretation, the satellites correspond to transitions to singlet (6 eV) and triplet (3 eV) states of the final $2p^53d^9$ configuration, split by the

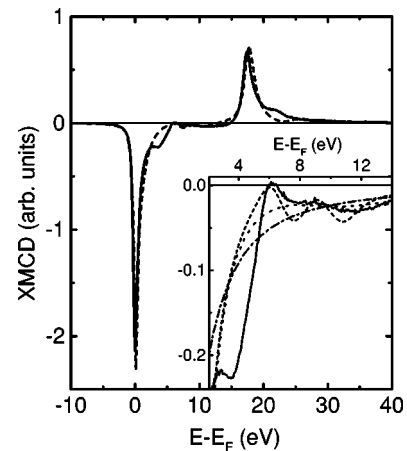


FIG. 2. $L_{2,3}$ edge XMCD, as calculated by RSMS theory (dashes) and from experiment (solid). Inset: L_3 edge XMCD (dashes) from theory and experiment (solid); theory for a cluster of 13 atoms (dots), and atomic background contribution to the XMCD signal (dash-dot).

core-valence exchange interaction. The singlet state cannot be reached from a triplet $3d^8$ initial state unless one allows spin-flip transitions due to the $2p$ spin-orbit interaction. A related investigation was conducted in case of photoemission.²¹ We believe, however, that the effect of spin-flip transitions is negligible in this case, and present evidence that the 6-eV satellite is predominantly a multiple scattering effect. For the 3-eV satellite, however, the multiplet explanation is reasonable, and its presence is indicative of limitations of one-electron theory.

Both the 6-eV feature in XANES and the zero in the XMCD signal at about 6 eV are correctly reproduced by our RSGF calculations. Within MS theory, these features can be viewed as the effect of multiple scattering from the environment (dashes in Fig. 2) on top of a smooth atomic background signal (dot-dash). The importance of multiple scattering in magnetic L -edge EXAFS of $3d$ elements was previously noticed.²³ From XMCD theory the XMCD signal is the difference in XAS between spin-up and spin-down components, i.e., $\mu^+ - \mu^-$. Thus zeros in XMCD can be interpreted as the energies where the spin-up density of states (DOS) is equal to spin-down DOS, while the extrema correspond to energies where the spin-up and -down DOS have the largest differences. Alternatively one can say that the XMCD signal is proportional to the derivative of the XAS, so the zeros of the XMCD correspond to peaks in the XAS.

It has been observed that the 6-eV feature disappears in the case of very thin films. This observation is consistent with our interpretation, and since it results from a reduction of the multiple-scattering contribution due to an effectively reduced cluster size (Fig. 2 inset, dots). Thus we feel that the disappearance of the negative spin polarization at about 6 eV seen in experiment is due to spin-dependent destructive interference from multiple scattering. The RSMS theory also predicts a small oscillation at about 8 eV above the L_3 edge in both the XAS and XMCD due to multiple scattering; however, experimental noise makes this feature difficult to observe conclusively.

The extended negative (positive) tail in the XMCD above L_3 (L_2) edges is well reproduced by RSMS calculations. The existence of such tails is not surprising within the derivative interpretation of XMCD. Since the atomic background absorption should become small at high energies, one expects to have smooth tails above L_3 (L_2) edges. In Fig. 2 it seems that the negative tail (plateau) between L_3 and L_2 edges is slightly more pronounced in experiment than in theory. However, this discrepancy might be due in part to overlap with L_2 edge, and theory allows one to disentangle these edges. The broadening of the L_2 theoretical spectrum with only the core-hole lifetime gives too big a signal in the region below the L_2 edge, and this in turn, kills the negative tail coming from the L_3 edge. So instead of looking at the combined L_2 and L_3 signals, it is probably better to consider only the L_3 edge, as shown in the inset to Fig. 2. One sees that the theoretical XMCD signal for the L_3 edge alone clearly has a negative tail that extends up to ~ 15 eV above the edge, and it is clear that this smooth signal is dominated by the atomic background contribution. A common explanation for the negative plateau between the L_3 and L_2 edges is the so-called “diffuse magnetism,”^{3,24} i.e., the contribution from delocalized s electrons. We tested this hypothesis using

RSMS calculations with only final d states (i.e., without s contributions), but did not see any difference within the line width in Fig. 2. This failure of the “diffuse magnetism” interpretation is perhaps not unexpected, at least for bulk systems. For bulk fcc Ni, s states can contribute as much as 7% to the total spin moment.²⁵ However, the matrix element for transitions to s states is about an order of magnitude smaller than that for transitions to d states. In addition, the matrix elements are smooth functions of energy and, as a result, the contribution from s states is evenly distributed in an extended energy range, and not just in a 5–10-eV interval between L_2 and L_3 edges. Therefore, we conclude that the observed negative plateau between L_3 and L_2 edges and, similarly, the extended positive tail above the L_2 edge is due to transitions to spin-polarized continuum ϵd states. Our RSMS calculations also show that the unoccupied part of the d density of states has long tails extending up to ~ 15 eV, i.e., much broader than one would expect for a single atom. For this reason, AM codes cannot reproduce them, even with substantial crystal fields. Such long tails in XANES are important for an accurate application of the sum rules, since the L_3 plateau is small, but not negligible near the main L_2 peak.

IV. CONCLUSIONS

Theoretical calculations can play an important role in the analysis of XANES and XMCD experiment, allowing one to disentangle various contributions to the experimental signal, e.g., one-electron and multielectron features, or transitions from p to s and from p to d states. We have shown that one-electron RSMS simulations for Ni L_3 edge XMCD and XAS reproduce all spectral features in experiment, with the notable exception of the 3-eV satellite. This feature has been traced to a multiplet effect, namely, singlet-triplet splitting, based on simulations with the AM code.¹⁴ The main white line peak in the spectra is clearly due to transitions to the unoccupied spin-down $3d$ states. The smooth background gives rise to a smooth plateau in XMCD, which is traced to transitions to delocalized ϵd states. The 6-eV peak is assigned to multiple scattering from the environment at intermediate range; indeed, three coordination shells are needed to simulate the peak. The zero in the XMCD signal at 6 eV is attributed to a cancellation between the central atom and multiple scattering contributions. Additional insight can be achieved by the observation that the $L_{2,3}$ XMCD is proportional to the difference in absorption between spin-up and spin-down electrons (neglecting small spin-orbit interaction in final state). With such an interpretation one immediately expects a smooth plateau from the central atom, and also rough proportionality of XMCD to the derivative of the XANES with energy. Although we have analyzed in detail only the XANES and XMCD for Ni, similar results are expected to hold for Co in Ni/Co films,²⁶ and in related materials.

ACKNOWLEDGMENTS

We thank F. de Groot, N. Martensson, A. Nilsson, G. Sawatsky, and J. Stöhr for useful comments. One of us (K.B.) thanks the SSRL for the hospitality extended to him during his stay. This work was supported in part by DOE Grant No. DE-FG03-98ER45718 and by UOP LLC.

- *Permanent address: Dept. of Physics, Freie Universität Berlin, Germany.
- ¹J. Stöhr, *J. Magn. Magn. Mater.* **200**, 470 (1999), and references therein.
- ²C.T. Chen, F. Sette, Y. Ma, and S. Modesti, *Phys. Rev. B* **42**, 7262 (1990).
- ³W.L. O'Brien and B.P. Tonner, *Phys. Rev. B* **50**, 12 672 (1994).
- ⁴D. Arvanitis, M. Tischer, J. Hunter Dunn, F. May, N. Mårtensson, and K. Baberschke, in *Spin-Orbit Influenced Spectroscopies of Magnetic Solids*, edited by H. Ebert and G. Schütz (Springer, Berlin, 1996), p. 259.
- ⁵P. Srivastava, N. Haack, H. Wende, R. Chauvistré, and K. Baberschke, *Phys. Rev. B* **56**, R4398 (1997).
- ⁶J. Vogel and M. Sacchi, *Phys. Rev. B* **53**, 3409 (1996).
- ⁷S.S. Dhesi, H.A. Dürr, G. van der Laan, E. Dudzik, and N.B. Brookes, *Phys. Rev. B* **60**, 12 852 (1999).
- ⁸F. Wilhelm, P. Pouloupoulos, P. Srivastava, H. Wende, M. Farle, K. Baberschke, M. Angelakeris, N.K. Flevaris, W. Grange, and J. -P. Kappler, *Phys. Rev. B* **61**, 8647 (2000).
- ⁹F. May, M. Tischer, D. Arvanitis, M. Russo, J. Hunter Dunn, H. Henneken, H. Wende, R. Chauvistré, N. Mårtensson, and K. Baberschke, *Phys. Rev. B* **53**, 1076 (1996).
- ¹⁰L.H. Tjeng, C.T. Chen, P. Rudolf, G. Meigs, G. van der Laan, and B.T. Thole, *Phys. Rev. B* **48**, 13 378 (1993).
- ¹¹N.B. Brooks, B. Sinkovic, L.H. Tjeng, J.B. Goedkoop, R. Hesper, E. Pellegrin, F.M.F. de Groot, S. Altieri, S.L. Hulbert, E. Shekel, and G.A. Sawatzky, *J. Electron Spectrosc. Relat. Phenom.* **92**, 11 (1998).
- ¹²M. Magnuson, A. Nilsson, M. Weinelt, and N. Mårtensson, *Phys. Rev. B* **60**, 2436 (1999), and references therein.
- ¹³T. Jo and G.A. Sawatzky, *Phys. Rev. B* **43**, 8771 (1991).
- ¹⁴F. de Groot, *J. Electron Spectrosc. Relat. Phenom.* **67**, 529 (1994), and references therein.
- ¹⁵H. Ebert, *Rep. Prog. Phys.* **59**, 1665 (1996).
- ¹⁶A.L. Ankudinov, B. Ravel, J.J. Rehr, and S.D. Conradson, *Phys. Rev. B* **58**, 7565 (1998).
- ¹⁷G.Y. Guo, *Phys. Rev. B* **57**, 10 295 (1998).
- ¹⁸N.V. Smith, C.T. Chen, F. Sette, and L.F. Mattheiss, *Phys. Rev. B* **46**, 1023 (1992).
- ¹⁹A.L. Ankudinov and J.J. Rehr, *Phys. Rev. B* **56**, R1712 (1997).
- ²⁰A.I. Nesvizhskii and J.J. Rehr, *J. Synchrotron Radiat.* **6**, 315 (1999).
- ²¹G. van der Laan, S.S. Dhesi, E. Dudzik, J. Minar, and H. Ebert, *J. Phys.: Condens. Matter* **12**, L275 (2000).
- ²²E.A. Stern and J.J. Rehr, *Phys. Rev. B* **27**, 3351 (1983).
- ²³H. Wende, P. Srivastava, D. Arvanitis, F. Wilhelm, L. Lemke, A. Ankudinov, J.J. Rehr, J.W. Freeland, Y.U. Idzerda, and K. Baberschke, *J. Synchrotron Radiat.* **6**, 696 (1999).
- ²⁴W.L. O'Brien, B.P. Tonner, G.R. Harp, and S.S.P. Parkin, *J. Appl. Phys.* **76**, 6462 (1994).
- ²⁵O. Eriksson, A.M. Boring, R.C. Albers, G.W. Fernando, and B.R. Cooper, *Phys. Rev. B* **45**, 2868 (1992).
- ²⁶S.S. Dhesi, H.A. Dürr, E. Dudzik, G. van der Laan, and N.B. Brookes, *Phys. Rev. B* **61**, 6866 (2000).